Chapter 2
Inherent Defying Features in Shale Gas Modelling

Abstract Accurate simulation and modelling of shale gas reservoirs are deemed crucial for efficient exploitation of these resources. Obtaining realistic results for resource estimation and performance predictions has a significant impact on the economics of the operating companies and all interested parties. Integrating all the unique characteristics of shale gas reservoirs within a single reservoir simulator for accurate predictions of future performance has become an increasingly intricate task. For many years now, various researchers have tried to tackle some of these challenges which include, but not limited to, how the natural fractures are simplified and represented in a simulator, the transport of gas within the matrix and fractures, adsorption and desorption phenomena within the shale gas system and also how the fractures are propagated within the shale formation upon hydraulic fracturing. This chapter provides an overview of the advances made in shale gas modelling and highlights the improved understanding conveyed by various researchers on the main defining characteristics of shale and the way these features of shale are modelled in numerical reservoir simulators.

2.1 Incorporation of Natural Fractures in Shale Gas Models

Natural fractures play an important role in the production of natural gas from shale gas reservoirs. Where these fractures are present, there must be an extensive network of the fractures intersecting to be able to contribute towards production of the natural gas. For instance, according to Walton and Mclennan (2013), the Devonian shale of the Appalachian basin is considered to be highly fractured with a fracture spacing of order 1–10 cm, whereas that of the Atrium shale of Michigan basin is more intensely fractured with fracture spacing of 1–2 ft.

Walton and Mclennan (2013) raised the question of whether these natural fractures, if present, is, in fact, open and if so, how they are maintained open against closure stress. According to the authors, if these natural fractures behave just like coal cleats, are they initially filled with water? And how much of this water

J. Gholinezhad et al., *Challenges in Modelling and Simulation of Shale Gas Reservoirs*, SpringerBriefs in Petroleum Geoscience & Engineering,
https://doi.org/10.1007/978-3-319-70769-3_2

production is actually observed? An assumption that they believed is commonly made is to assume that the fractures are open and gas filled.

The contribution of open natural fractures to economic gas production is perceived to be because of their large surface area. However, Walton and Mclennan (2013) argued in their paper that the contribution of this large surface area to gas production is possible only for the ultra-low-permeability shallow gas shales, whereas a much smaller surface area would be required for the deeper gas shales such as Barnett. The Barnett shale, in particular, is believed to have less natural fractures as it is often argued that the abundance of open natural fractures would have resulted in the expulsion and migration of the gas out of the shale into overlying rocks. Other arguments seek to suggest that the prolific abundance of natural gas within the Barnett shale could only be as a result of the presence of open natural fractures.

The storage capacity of the matrix is much higher than that of the fractures, and in many of the shale gas reservoirs, the fractures tend not to hold any gas at all. Bai et al. (1993) argued that the storage capacity of a fractured system should not always be considered negligible compared to the storage of the matrix. This is because, in most reservoirs that experience a high degree of production initially, most of the gas must have been stored in the fractures and hence there is always a drastic decline after a short period of time.

The open fractures may, however, be filled by fracturing fluid used in the hydraulic fracturing process. The permeability of the matrix is lower relative to that of the fractures.

There are basically two methods used in characterising fractured reservoirs. These are dual porosity/dual permeability models and discrete fracture network models.

2.1.1 Dual Porosity/Dual Permeability Model

Naturally fractured reservoirs are characterised by the presence of two distinct porous media, the matrix and fractures. Naturally fractured reservoirs have been referred to as dual porosity system as a result of the two porous media which are present (Barenblatt et al. 1960). The matrix feeds fluid locally to the fractures, and the fractures form a continuous system connected to the well.

Under the dual porosity model which was further modified by Warren and Root (1963), the matrix does not contribute directly to the wellbore. The system was seen as an orthogonal set of intersecting fractures and sugar cubic matrix block (Fig. 2.1), and by using differential equations, analytical solutions were obtained for well test analysis.

Warren and Root (1963) assumed flow from the matrix to the fracture occurs under a transfer function with Darcy characteristics and also flow occurs under pseudo-steady state conditions in the matrix blocks with a single value assigned to the pressure in the blocks. The pressure differential between the matrix and the

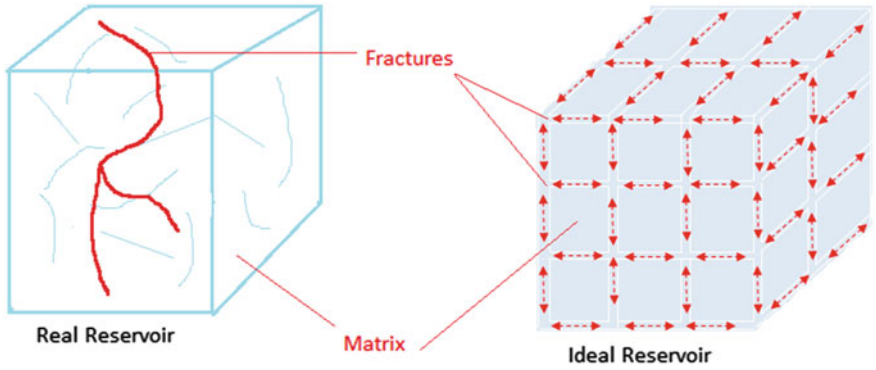

Fig. 2.1 Sugar cube model by Warren and Root

fractures, therefore, determines the mass transfer rate of the fluid. Thus, the inter-porosity flow has been described by two main mechanisms which are the pseudo-steady state and the transient flow. Warren and Root (1963) predicted that on a semi-log plot of the test data, two parallel straight lines will develop. The slope of the parallel lines represented the flow capacities of the formation, whereas the vertical separation of the lines represented the storage capacity of the fractures. This is shown in Fig. 2.2.

Odeh (1965) developed a simplified model with mathematical equations that described the unsteady state behaviour of fractured reservoirs. He concluded from his studies that there was no difference between fractured reservoir and

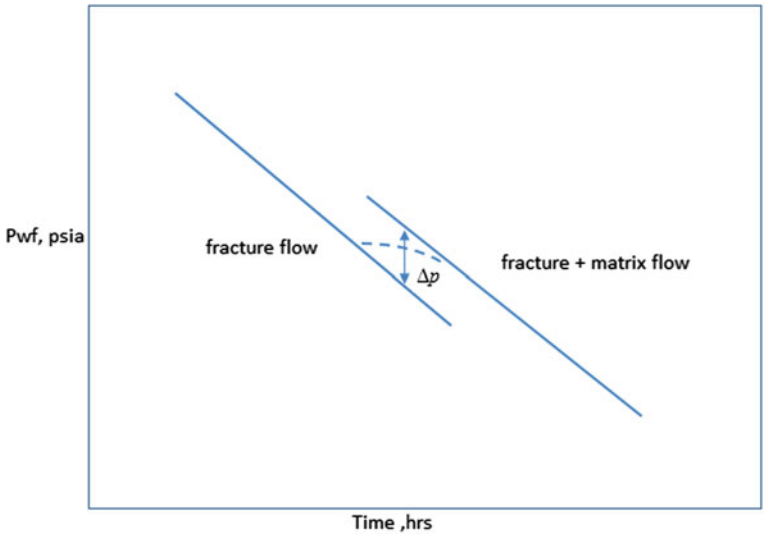

Fig. 2.2 Pseudo-steady state matrix flow pressure build-up curve (Warren and Root 1963)

homogeneous reservoir on the basis of drawdown and build-up curves using field measured data. This according to Kazemi (1969), contradicted the results of Warren and Root (1963) but with smaller block dimensions and a higher permeability, their results remain valid. Odeh (1965) used a similar model as Warren and Root (1963) although his results did not show the two parallel straight lines as depicted in Fig. 2.2.

The dual porosity model by Warren and Root (1963) was extended to include transient flow in the matrix block by Kazemi (1969). The main distinction for Kazemi (1969) was the use of transient flow within the matrix instead of assuming a pseudo-steady state as was done by Warren and Root (1963). Kazemi (1969) also used the slap model (sheets of parallel fracture sets) (Fig. 2.3) to describe the reservoir. By considering a direct flow to the well, he found that similar results to Warren and Root (1963) were obtainable without affecting the results in any sensible way, except for a smooth transitional zone which occurs due to the non-permanent flow regime of the fluid flow from the matrix to the fractures. Thus, deviations will occur in the transitional period when the rock matrix is described by a pseudo-steady state regime.

de Swaan (1976) expanded on the dual porosity model by using transient flow as the basis of flow from the matrix to the fractures. He defined his transient model by intrinsic properties of the matrix and the fractures as opposed to the bulk properties of the matrix and fractures used by both Warren and Root (1963) and Kazemi (1969). Both slab matrix shape model and a spherical matrix block solution were also presented in the same study.

Serra et al. (1983) also used the transient model to describe the fluid flow from the matrix to the fractures and based his model on intrinsic properties rather than bulk properties. Serra et al. (1983) model was very similar to de Swaan (1976) except for the use of different storativity ratio and inter-porosity coefficient.

Najurieta (1980) showed in a simplified description the pressure behaviour of naturally fractured reservoir based on appropriate solutions of the de Swaan

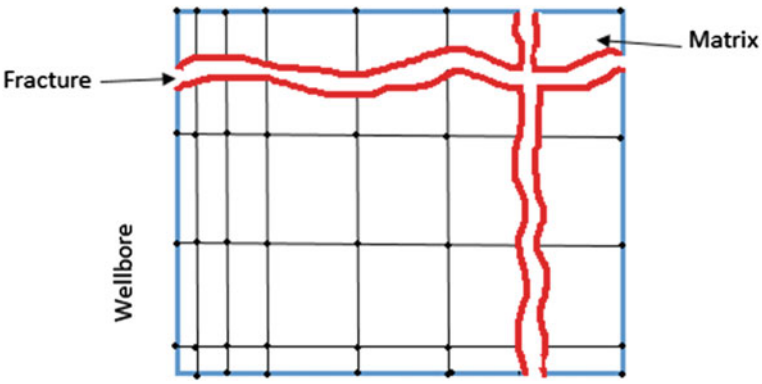

Fig. 2.3 Dual porosity idealisation by Kazemi (1969)

differential equation. In his study, he deduced equations that properly described the transitional period taking into account the unsteady state behaviour of the matrix. He also showed that the behaviour of a uniformly fractured reservoir can be fully described by four parameters each of which is a function of two or more of the five basic reservoir parameters (fracture and matrix porosity, fracture and matrix permeability and fracture spacing).

2.1.2 Discrete Fracture Network

DFN relies more on the spatial mapping of the fractures to construct an interconnected network of the fractures. It is seen as a more recent development.

According to Dershowitz et al. (2004), DFN may be defined as an analysis and modelling which explicitly incorporates the geometry and properties of the discrete features as a central component controlling flow and transport. The equation of flow is solved on each individual fracture network (McClure and Horne 2013).

One distinction between DFN and continuum model is that continuum model averages fracture properties into effective properties over volumetric grid blocks.

McClure and Horne (2013) discussed the benefit of using DFN in describing the complex nature of the fracture networks in low-permeability medium. With low-permeability rocks, individual fractures in close proximity with no intersection are mostly not well connected. Due to this, fluid flow between the locations will depend on the nature of the fracture network geometry. Sometimes more distant fractures provide a better connectivity than closer fractures (McCabe et al. 1983; McClure and Horne 2013).

Also, another useful benefit of using DFN is that stresses in the rock can be handled more accurately. According to McClure and Horne (2013), stresses caused by fracture opening or sliding are very heterogeneous spatially and its effect on neighbouring fractures is dependent on their relative orientation and location. There are two main types of DFN used: deterministic model and stochastic model.

The deterministic model defines explicitly the location, orientation and dimensions of the individual fracture which is then included in the model. The challenge with this modelling is the fact that for a complex system of fractures, it will be impossible to define accurately the location and properties explicitly of each of the fractures within the reservoir.

Stochastic models analyse certain properties of the fracture such as fracture height, length, aperture, orientation and spacing together with some statistical scaling rule that defines the fracture architecture. A statistical approach is adopted where the properties of the fracture system are generated randomly. To have an accurate representation of the flow system, many realisations of the fracture network flow system will have to be simulated.

According to Herbert (1996), it is not always possible in practice to simulate efficiently many realisations and often more qualitative bounds are estimated from a smaller sample of model results.

2.2 Diffusion Models in Shale

One of the key characteristics of shale gas reservoirs is the flow of gas in the pore network. The pores of shale gas reservoirs are within the ranges of 1–200 nm (Lee and Kim 2015).

Javadpour et al. (2007) conducted experiments on 152 core samples from nine shale reservoirs and reported that the average permeability of shale gas reservoirs is of the range 54 nD (5.43×10^{-20} m^2).

The flow of gas within this nano-pore is essential for gas production as well as accurate simulations of shale gas reservoirs. Due to the nano-pores of the reservoir, the apparent permeability is mostly dependent on the pore pressure, fluid type and the pore structure (Guo et al. 2015).

In conventional reservoirs flow is continuous, whereas in shale gas reservoirs gas can flow in the nano-pores in the slip flow regime, the transitional regime and the molecular regime in addition to the continuum regime (Geng et al. 2016).

Darcy's law which is used in conventional reservoirs to capture continuum flow regimes is inadequate to describe other flow regimes that occur in the nano-pores.

The nature of the nano-pores, therefore, plays a significant role in the dynamics of the fluid flow and its interactions with the surfaces of the shale. These are different from conventional reservoirs where the pore network is much bigger and flow can easily be described by Darcy's law. The application of Darcy's law in nano-pores of the shale reservoirs will only underestimate the flow rate, thus conventional Darcy's law is not applicable in shale gas reservoirs and caution must be exercised whenever it is used.

Under certain pressure and temperature conditions, the mean free path might exceed the size of the pores and this might cause the gas molecules to move singly through the pores. When this happens, the concept of continuum or bulk flow may not be applicable (Lee and Kim 2015).

The gas diffusing through a porous media may involve collisions between the gas molecules as well as collisions between the gas molecules and the walls of the porous media.

The flow of fluid within any porous medium can be distinguished using the Knudsen number. The Knudsen number is the ratio of the gas mean free path to the diameter of the pore size.

$$K_n = \frac{\lambda}{d_p} \tag{2.1}$$

where d_p is the diameter of the pores and λ is the gas mean free path. A K_n greater than 10 implies collision between gas molecules and the walls of the porous media. Knudsen diffusion is dominant in such case with negligible molecular diffusion and viscous diffusion. If K_n is much smaller than 0.1, collisions and interaction of the gas molecules become dominant and Knudsen diffusion becomes negligible compared with molecular and viscous diffusion.

Table 2.1 Flow regimes with corresponding Knudsen number

Knudsen number	Flow regime
(a) 0–10^{-3}	Continuum/Darcy flow (no-slip flow)
(b) 10^{-3}–10^{-1}	Slip flow
(c) 10^{-1}–10^{1}	Transition flow
(d) 10^{1}–∞	Free molecule flow

Rathakrishnan (2013) presented a table of different flow regimes corresponding to Knudsen numbers (see Table 2.1).

For Knudsen number between 0 and 10^{-3}, the continuum assumptions are valid and flow can be described by the Navier–Stokes (N–S) equations with no-slip boundary conditions. However, for Knudsen number between 10^{-3} and 10^{-1}, the flow can be described as slip flow and N–S equations become invalid. For Knudsen number between 10^{-1} and 10^{1}, flow is said to be in the transitional region between slip and free molecule flow and finally with Knudsen number greater than 10, the free molecular regime is encountered with collisions between the gas molecules and the walls of the media dominating (see Fig. 2.4).

Collisions of the gas molecules with the walls of the porous media are predominant especially for shale gas reservoirs due to the nano-pores which also makes permeability measurement a challenge. There are, however, negligible collisions between the gas molecules themselves compared with the collisions with the wall surfaces of the media. For typical shale gas reservoirs, the Knudsen number ranges from 2×10^{-4} to 6.0. As shown in Fig. 2.5, the slip flow occurs for most pore sizes at the initial reservoir pressure. With the pore pressure decreasing, the transition flow generally becomes dominant.

In such cases, the use of N–S equations is no longer valid. These equations are derived from the basic principles of conservation of mass, conservation of energy and conservation of momentum. It is based on the assumption that the fluid is a continuum, that is, it is not made up of discrete particles but rather a continuous substance.

According to Gad-el-hak (1999), the N–S model ignores the molecular nature of gases and liquids and regards the fluid as a continuous medium describable in terms of the spatial and temporal variations of density, velocity, pressure, temperature and other macroscopic flow quantities. The assumption of N–S can only be valid when the three fundamental assumptions of Newtonian framework (fluid with Newtonian viscosity), continuum approximation (mean free path much less than flow conduit dimensions) and thermodynamic equilibrium are satisfied (Gad-el-hak 1999; Moghaddam and Jamiolahmady 2016).

N–S equation has been modified by various other researchers to account for slip boundary condition. Other models have been developed to address the flow of fluid in a media at the molecular level when the N–S equations become invalid. These models are, however, excessively time-consuming and unrealistic to simulate gas flow. They include molecular dynamic (MD), direct simulation Monte Carlo (DSMC) or solution of linearised Boltzmann equation (LBE).

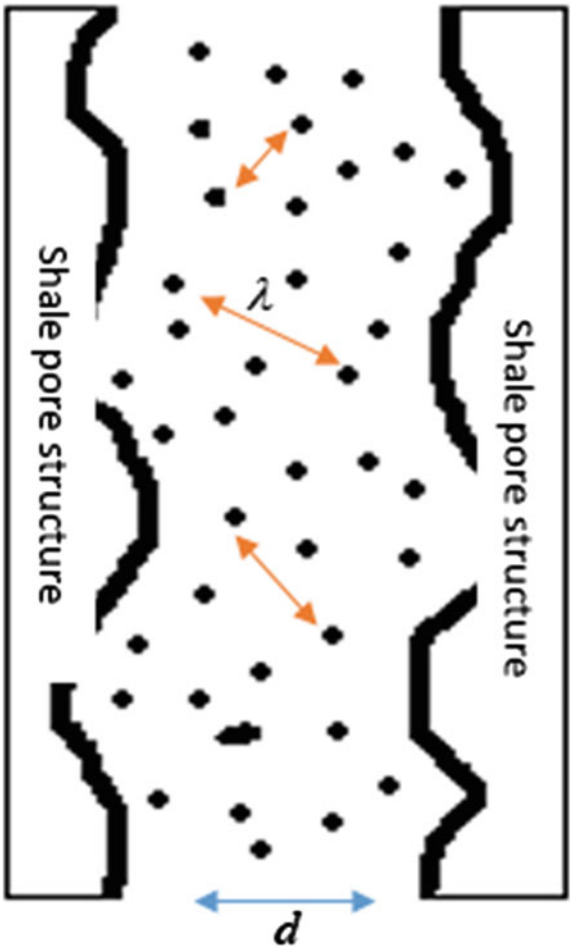

Fig. 2.4 Flow within a shale pore structure with gas molecules collisions

There have been a number of methods which accounts for slip boundary condition such as the Maxwell slip and second-order slip. Maxwell slip condition is a first-order approximation from the kinetic theory of gases and its being widely applied to predict the mass flow in micro- and nano-channels.

For a complete description of the flow in tight media, the model developed should be able to account for Knudsen diffusion as well as slip flow and the processes of adsorption and desorption. Thus, gas flow through shale nano-pores has been described by several models that account for Knudsen diffusion, slip flow and desorption.

Klinkenberg (1941) conducted experiments to explain the phenomenon of gas transport through porous media. He concluded that gas permeability is a function of mean pressure and gas composition and that the equivalent liquid permeability is independent of both mean pressure and gas composition. He showed that a linear

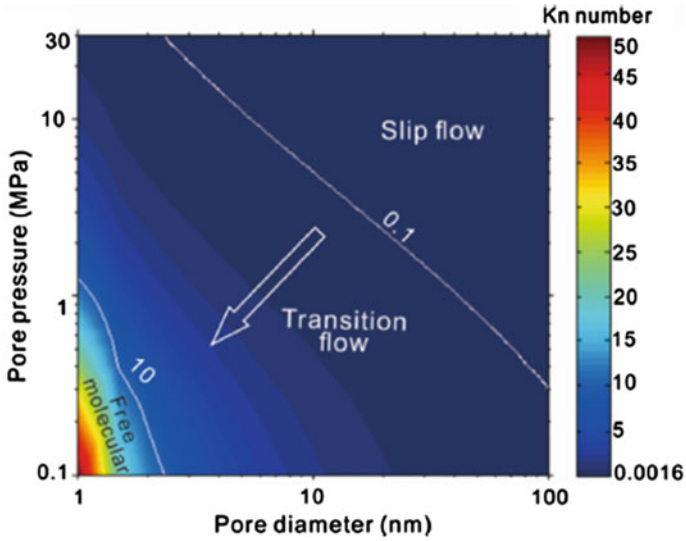

Fig. 2.5 Contour plot of the Knudsen number versus pore pressure size (Geng et al. 2016). Slip flow occurring at initial reservoir pressure

relationship exists between the Darcy permeability and the reciprocal of the mean pressure of the system.

$$k(p_{\text{avg}}) = k_{\text{D}}\left(1 + \frac{b}{p_{\text{avg}}}\right) \tag{2.2}$$

where $k(p_{\text{avg}})$ is the gas permeability at mean pressure p_{avg}, k_{D} the Darcy permeability or liquid permeability and b the Klinkenberg parameter. Conventional gas reservoirs have been modelled with the Klinkenberg effect, and recent use has been made for tight gas reservoirs with pores of 1–10 μm in size. Thus, slippage effect of the gas molecules can be accounted for when using Klinkenberg's model.

Javadpour (2009) developed a new model that accounted for a no-slip boundary and Knudsen diffusion using Maxwell theory. The new model presents an equation that is derived from the theoretical basis as in molecular dynamics but written in a format compatible with the Darcy equation. According to Javadpour (2009), this can be easily incorporated into commercial reservoir simulators to study gas production from mud rock systems. Javadpour (2009) model converges to the Knudsen diffusion model when the average pore size decreases and when the sizes increases, it converges to the continuum model.

$$k_{\text{app}} = \frac{2r\mu}{3 \times 10^3 p_{\text{avg}}}\left(\frac{8\text{RT}}{\pi M}\right)^{0.5} + \frac{r^2}{8}\left\{1 + \left(\frac{8\pi\text{RT}}{M}\right)^{0.5}\left(\frac{2}{\alpha} - 1\right)\frac{\mu}{rp_{\text{avg}}}\right\} \tag{2.3}$$

k_{app} is the apparent permeability for a porous medium in a straight cylindrical nanotube. The apparent permeability relationship with Klinkenberg can be written in the form

$K_{app} = k_D\left(1 + \frac{b}{p_{avg}}\right)$, where b is given as

$$b = \frac{16\mu}{3 \times 10^3 r}\left(\frac{8RT}{\pi M}\right)^{0.5} + \left(\frac{8\pi RT}{M}\right)^{0.5}\left(\frac{2}{\alpha} - 1\right)\frac{\mu}{r}, \tag{2.4}$$

This model is simple as it assumed an ideal gas and no desorption.

Azom and Javadpour (2012) corrected the above equation to account for real gas flowing in a porous medium. The final modified equation remained the same as above with b given as

$$b = \frac{16\mu c_g p_{avg}}{3 \times 10^3 r}\left(\frac{8ZRT}{\pi M}\right)^{0.5} + \left(\frac{8\pi RT}{M}\right)^{0.5}\left(\frac{2}{\alpha} - 1\right)\frac{\mu}{r} \tag{2.5}$$

to account for the gas compressibility factor. As the gas becomes ideal, Eq. (2.2) changes to Eq. (2.1) since the gas compressibility $c_g = \frac{1}{p_{avg}}$ and $Z = 1$.

Civan (2010) developed a model under slip flow assumptions represented by second-order slip approximations. This was based on Beskok and Karniadakis (1999) model of rarefied gas flow in a micro-channel, ducts and pipes. The model assumes that permeability is a function of the intrinsic permeability, the Knudsen number, the rarefication coefficient and the slip coefficient. Thus,

$$k = k_D(1 + \alpha_r k_n)\left(1 + \frac{4k_n}{1 - bk_n}\right) \tag{2.6}$$

with rarefication coefficient given as:

$$\alpha_r = \alpha_0\left(\frac{K_n^B}{A + K_n^B}\right) \tag{2.7}$$

The drawbacks of this model are the use of several empirical parameters which require performing several experiments.

Darabi et al. (2012) formulated a pressure-dependent permeability function known as apparent permeability function (APF). The APF model describes gas flow in ultra-tight natural porous media characterised by a network of interconnected tortuous micro-pores and nano-pores. Darabi et al. (2012) adapted the model developed by Javadpour (2009) to include surface roughness as well as Knudsen diffusion and slip flow (Maxwell theory). The APF in porous media is given as:

$$k_{\text{app}} = \frac{\mu M}{\text{RT}\rho_{\text{avg}}} \frac{\phi}{\tau} (\delta')^{D_f - 2} D_{\text{k}} + k_{\text{D}} \left(1 + \frac{b}{p}\right) \tag{2.8}$$

D_{k} is the Knudsen diffusion coefficient and δ' is the ratio of normalised molecular size (d_{m}) to local average pore diameter (d_{p}), $\delta' = d_{\text{m}}/d_{\text{p}}$. R_{avg} is the average pore radius, approximated by $R_{\text{avg}} = (8k_D)^{0.5}$.

Singh and Javadpour (2016) proposed a different approach to modelling apparent permeability in shale gas reservoirs. This approach deviated from the empirical approach used by earlier researchers. The term non-empirical apparent permeability (NAP) is used to describe this model which is an analytical equation that depends on the pore size, pore geometry, temperature, gas properties and average reservoir pressure. The NAP model was derived without the assumption of slip flow at the pore walls. The proposed model also showed that the pore surface roughness and mineralogy have negligible influence on gas flow rate under a complete range of reservoir operating conditions. Singh and Javadpour (2016) model accounts for both Knudsen diffusion and sorption in a porous medium but ignores slip flow.

Singh and Javadpour (2015) extended the analytical model for apparent permeability determination in shale gas reservoirs by developing a new permeability model that goes away with the shortcomings of Maxwell slip condition, uses readily available Langmuir sorption data to determine the slip coefficient for gas flow and also includes a higher-order slip effect on gas flow. This model is referred to as the Langmuir slip permeability (LSP). The LSP is based on the Langmuir slip condition of Myong (2003) which considers the gas surface molecular interactions.

Geng et al. (2016) developed a new model for gas flow based on the extended Navier–Stokes equations without adsorption and desorption. The model takes into account all the possible flow regimes including continuum regime, slip flow regime, the transitional regime and molecular regime. However, without incorporating the adsorption or desorption component, this model falls short in capturing the real phenomena of the flow process in the nano-pores.

A finite difference method called finite difference geometrical pore approximation (FDGPA) was introduced by Shabro et al. (2012) to simulate pore scale fluid flow in a porous media. In this model, geometrical parameters are defined in interstitial space domain to characterise pore scale images. This method is relatively six times faster on average than the Lattice Boltzmann method (LBM) which requires significant computational effort.

Comparison of different models describing fluid flow in porous media together with the pros and cons has been summarised by Singh and Javadpour (2015) in Fig. 2.6 and Table 2.2.

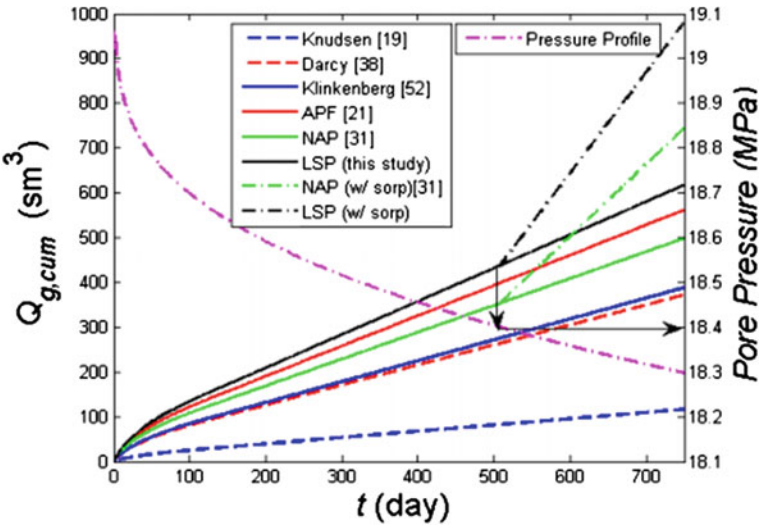

Fig. 2.6 Comparison of different models to predict cumulative gas production (Singh and Javadpour 2015)

2.3 Modelling of Fracture Propagation

In shale gas reservoirs, low permeability of shale implies very little or no recovery of gas through conventional drilling. Thus, to initiate flow to the wellbore, complex network of fractures are required to allow the gas to flow through them and into the well for production. Hydraulic fracturing is the key in creating these fractures that allow for an increase in the permeability to assist in fluid flow.

There is, therefore, the need to understand how these fractures will propagate through the formation. Various analytical and numerical techniques have been developed to model fracture propagation in shale gas reservoirs. These models are sometimes incorporated into reservoir simulators to assist in predicting shale gas performance.

Modelling of hydraulic fractures requires the application of three fundamental equations which are the continuity equation, momentum or fracture fluid flow and the linear elastic fracture mechanics (LEFM).

Both the continuity equations together with the fluid flow are coupled using a relation between the fracture width and fluid pressure, whereas the resulting deformation is modelled through LEFM.

2D modelling techniques were first to be used in modelling the fracture propagation; however, these models require the use of several assumptions that limit their use. The development of planar 3D and pseudo-3D models has helped to bridge this limitation while allowing for easier computational analysis.

All of these models require the understanding of the fracture geometry which includes the height of the fracture, its length and also the width. Commonly used

Table 2.2 Summary of models for diffusion in shale gas (Singh and Javadpour 2015)

Model	Description	Pros	Cons
Javadpour (2009)	Model developed using slip assumption, represented by Maxwell theory. Accounts for Knudsen diffusion. Modelled only for straight capillary tubes	Simple	Limited to straight tubes ideal gas. Ignores desorption
Civan (2010)	Model developed using slip flow assumption, represented by simplified second-order slip model. Contains several empirical parameters	Higher-order slip flow	Several empirical parameters
Darabi et al. (2012)	Model developed using slip flow assumption. Represented by Maxwell theory. Accounts for surface roughness and Knudsen diffusion in a porous medium	Includes tortuosity and pore surface roughness	Needs TMAC values. Ideal gas ignores desorption
Akkutlu and Fathi (2011)	Model includes dual porosity continua of matrix/fracture system where the matrix is composed of both organic and inorganic pores. Accounts for surface diffusion in a porous medium	Dual porosity system	Complex numerical model
Shabro et al. (2012)	A finite difference-based numerical model and geometrical parameters are used to reconstruct the porous structure of shale, which is then used for pore scale characterisation. Permeability equation is borrowed from Javadpour 1	Spatial characterisation and geometry of porous media included	Complex numerical model. Ideal gas ignores desorption. Needs TMAC values
Sakhaee-pour and Bryant (2011)	Model developed using slip flow assumptions, represented by Maxwell theory. Accounts for Knudsen diffusion	Spatial characterisation and geometry of porous media included	Needs TMAC values. Ideal gas
Mehmani et al. (2013)	Model developed by employing flow equation from Javadpour in pore network interconnected on Nano and micro length scales	Spatial characterisation and geometry of porous media included	Complex numerical model. Ideal gas. Ignores desorption. Needs TMAC values

(continued)

Table 2.2 (continued)

Model	Description	Pros	Cons
Singh and Javadpour (2016)	Model developed using Navier–Stokes equation and kinetic theory (no-slip flow assumption). Accounts for Knudsen diffusion, porous medium and sorption	Simple. No empirical coefficient	Ignores slip flow
Rezaveisi et al. (2014)	Numerical model developed to study components of produced gas with time from nanometre-sized pores. Relevant physics includes advection, slip flow and Knudsen diffusion	Distinguishes different gas types	Needs TMAC values
Kelly et al. (2015)	The porous structure of shale is reconstructed using FIB-SEM image stacks and numerical study using LBM is performed to study petro-physical properties of shale. Permeability estimation is done using pressure driven flow	Spatial characterisation and geometry of porous media included	Complex numerical model. Ignores slip, diffusion, and desorption
Chen et al. (2015)	The porous structure of shale is constructed using Markov Chain Monte Carlo (MCMC) on SEM images and its pore scale characterisation is performed. Apparent permeability includes flow from advection. Knudsen diffusion and slip. LBM is used to simulate fluid flow	Spatial characterisation and geometry of porous media included	Complex numerical model. Ignores desorption. Several empirical parameters
Naraghi and Javadpour (2015)	Model developed by stochastically characterising organic and inorganic pores. Accounts for slip flow. Knudsen diffusion, surface roughness and desorption	Distinguishes different pore systems in the organic and inorganic matter. Real gases	Needs additional information from SEM images. Needs TMAC values
Singh and Javadpour (2015)	Model developed using Langmuir slip condition and it does not carry several shortcomings associated with the use of Maxwell slip. Reliably predicts apparent permeability in shale	Simple and analytic. Gets slip coefficient from sorption data. Real gas	Ignores local heterogeneity

2D models include Perkins-Kern-Nordgren (PKN), Khristianovic-Geertsma-de Klerk (KGD) and circular fracture model.

Howard and Fast (1957) developed a mathematical model for fracture treatment which assumed the fracture width to be constant everywhere. A growing number of other 2D models have been developed since such as PKN and KGD. Usually with a 2D model, the fracture height is normally fixed and the fracture width and length will then be calculated.

Perkins and Kern (1961) developed the PKN model with modifications by (Nordgren 1972) to account for fluid loss. This model is usually used when the fracture length is greater than the fracture height or when there is a large length/height ratio. There are a number of assumptions that need to be satisfied for this model to be used successfully. These assumptions are best summarised by Nordgren (1972), Yew et al. (2015):

1. The fractures are assumed to be in a plane strain state in the vertical plane,
2. The vertical cross section is elliptical,
3. Fracture toughness has no effect on the fracture geometry since the energy needed for the fracture to propagate is less than that required for the fluid to flow along the fracture length,
4. Vertical fracture propagation in a straight line from the well,
5. Restricted vertical height,
6. Fracture is in plane strain in the vertical,
7. Isotropic, homogeneous, linear elastic rock mass.

PKN model is mostly used for long fractures with limited height and elliptical vertical cross section. The elliptical shape of the fracture propagation implies the width is not constant along the fracture height and length.

From Fig. 2.7, the maximum fracture width occurs where the fracture wing touches the wellbore and this width is a function of a distance from the wellbore.

$$x_{\mathrm{f}} = 0.68\left[\frac{GQ_o^3}{(1-v)\mu h_f^4}\right]^{1/5} t^{4/5} \tag{2.9}$$

$$w_0 = 2.5\left[\frac{(1-v)\mu Q_o^2}{Gh_f}\right]^{1/5} t^{1/5} \tag{2.10}$$

$$p_{\mathrm{w}} = \sigma_3 + 2.5\left[\frac{G^4\mu\, Q_o^2}{(1-v)^4 h_f^6}\right]^{1/5} t^{1/5} \tag{2.11}$$

where x_{f} is the fracture half length, w_0 is the maximum fracture opening, p_{w} is the wellbore pressure, G is the shear modulus, Q is the fluid injection rate, μ is the fluid viscosity and t is the time.

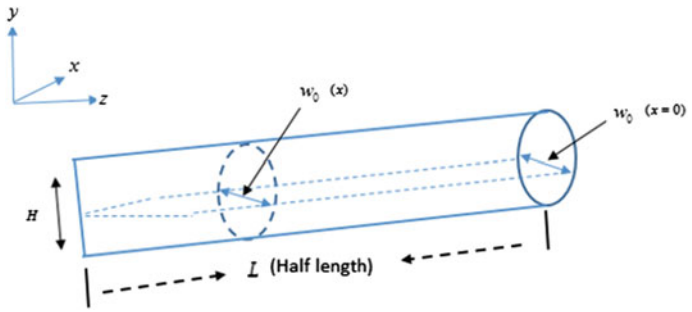

Fig. 2.7 Schematic model of PKN [modified from frackoptima.com ([1]http://www.frackoptima.com/userguide/theory/pkn.html)]

The KGD model is independent of height for width calculation and used often for very short fractures where plane strain assumptions are only applicable to horizontal sections (Adachi et al. 2007). Thus, KGD models are used when the fracture height is more than the fracture length. The geometry used in developing KGD model is illustrated in Fig. 2.8. The main assumptions under which KGD model is valid according to Geertsma and De Klerk (1969) are:

1. Vertical fracture propagating in a straight line from the well,
2. Restricted fracture height,
3. Homogeneous, isotropic, linear elastic rock mass,
4. Purely viscous fluid in laminar flow regime,
5. Rectangular vertical cross section of fracture,
6. Plane strain conditions in the horizontal plane.

Since the fracture is assumed to be at a plane strain condition in the horizontal plane, the KGD model is best suited for fractures whose length/height ratio is less or near unity (Yew et al. 2015).

$$x_{\mathrm{f}} = 0.48\left[\frac{8GQ_o^3}{(1-v)\mu h_f^4}\right]^{1/6} t^{2/3} \tag{2.12}$$

$$w_0 = 1.32\left[\frac{8(1-v)\mu Q_o^3}{G}\right]^{1/6} t^{1/3} \tag{2.13}$$

$$p_{\mathrm{w}} = \sigma_3 + 0.96\left[\frac{2G^3\mu Q_o}{(1-v)^3 x_f^2}\right]^{1/4} \tag{2.14}$$

Daneshy (1973) extended the KGD model for the case of power-law fluids or non-Newtonian fluids. He argued that the inclusion of non-Newtonian fluids allows

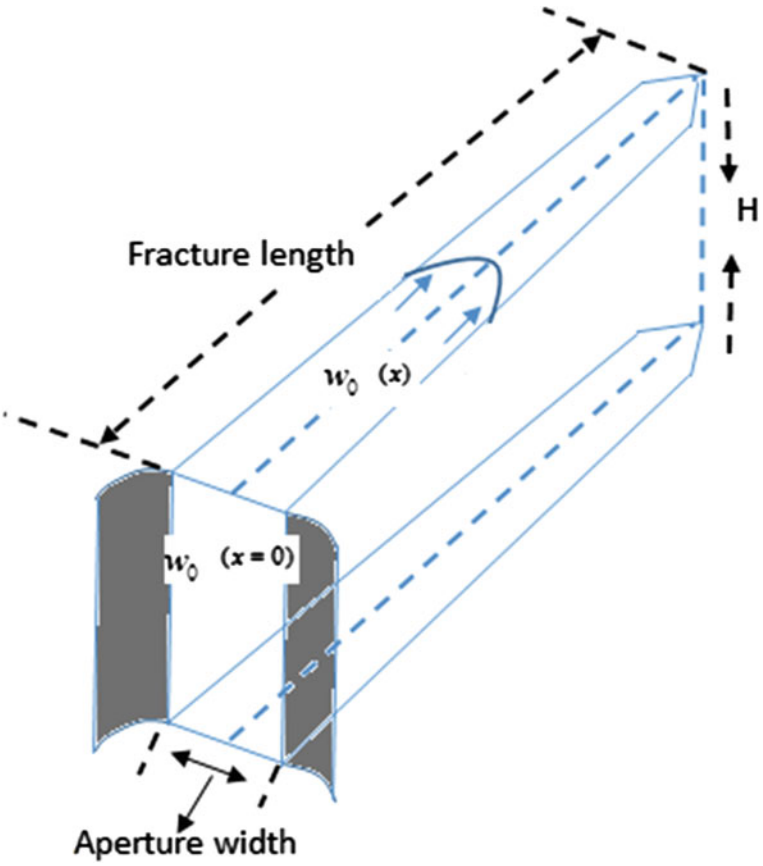

Fig. 2.8 Model geometry of KGD (modified from Weng 2015)

a more accurate consideration of most industrial fluids. By critically examining the assumptions involved in designing vertical hydraulic fractures, they found that some of these assumptions greatly affected the end results and that their presence does not necessarily affect the solution of the problem and their validity has not been tested. This was done on the basis of a new width equation and a numerical design procedure.

Settari and Cleary (1986) were the first to develop a pseudo-three-dimensional model (P3D) to describe the varying geometry of a 3D hydraulic fracture. According to Adachi et al. (2007), P3D is a crude yet effective attempt to capture the physical behaviour of planar 3D hydraulic fractures at minimal computational cost. Though this method might not be as accurate as numerical simulators, it requires less computing time and hence less expensive to develop. The P3D model does not consider the varying nature of the fracture geometry but instead modifies

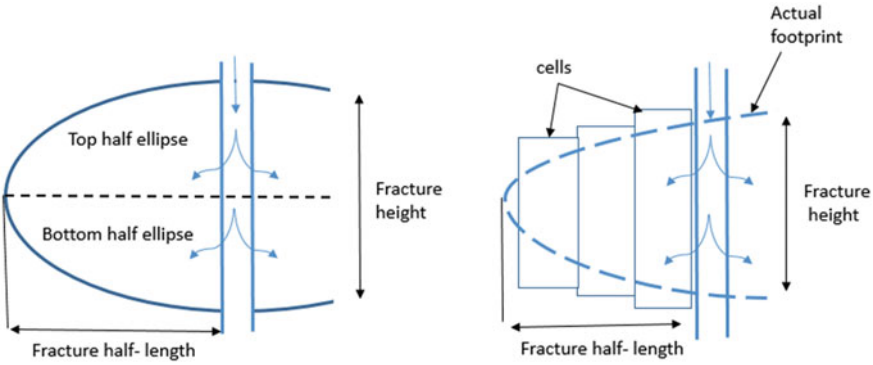

Fig. 2.9 Schematics showing fracture geometry based on 3D lumped elliptical model (**a**) and cell-based pseudo-3D geometry (**b**) (adapted from Weng 2015)

the 2D models by adding the varying height along the fracture length and its effect on the fracture width (Rahman and Rahman 2010). There are two types normally considered: lumped and cell-based (Mack and Warpinski 2000). The lumped model assumes that the vertical profile of the fracture consists of two half ellipses joined at the centre (Fig. 2.9a), whereas the cell-based models treat the fracture as a series of connected cells (Fig. 2.9b).

Though 2D models are simple, they are limited in that they require fracture height to be specified by the engineer and also by assuming that a radial fracture will develop. Another limitation is the fact that the fracture height is never the same especially from the well to fracture tip. The use of planar 3D models and pseudo-3D models has therefore been designed to address these limitations.

With respect to the planar three-dimensional models, the fracture geometry is defined by its width and the shape of its periphery which is, in turn, specified by the height at any distance from the well and length (Mack and Warpinski 2000). Planar 3D models describe the fracture propagation using either a 2D mesh of cells, either a triangular mesh or a fixed rectangular mesh. Planar 3D models have been developed also to address some of the limitations encountered when using the P3D models. An example of these limitations is that when there is an unconfined height growth, the P3D model tends to break down numerically.

2.4 Adsorption and Desorption Models in Shale

The composition of gas in shale gas reservoir is thought to be primarily made up of free gas stored within the pore network of the matrix and fractures and adsorbed gas on the surfaces of the shale matrix. The adsorbed gas is believed to be in the organic matter (kerogen).

Clarkson and Haghshenas (2013) outlined multiple mechanisms for gas storage in coals and in organic-rich shales. These are:

1. Adsorption upon internal surface area,
2. Conventional (compressed gas) storage in natural and hydraulic (induced) fractures,
3. Conventional storage in matrix porosity (organic and inorganic),
4. Solution in formation water,
5. Adsorption (solution) in organic matter.

The adsorption capacity of shale gas depends on a number of factors such as specific surface area, pressure, temperature, pore size and sorption affinity (Leahy-dios et al. 2011).

Total amount of gas in place is strongly affected by the TOC, clays and the adsorption ability of methane on the internal surface of the solid (Martin et al. 2010; Yu et al. 2014). Organic matter in shale is considered to have a strong adsorption potential due to its large surface area and its affinity to methane (Yu et al. 2014, 2015).

In shale gas reservoirs, the adsorption process is mainly considered to be a physical process such that both adsorption and desorption of gas molecules are reversible.

There are basically six different types of adsorption which the international union of pure and applied chemistry (IUPAC) has classified. Of the six categories, adsorption on shale gas reservoirs is normally classified under the Type I, also known as the Langmuir isotherm. The adsorption behaviour of the gas in shale gas reservoirs is normally described by the monolayer Langmuir isotherm. This means a single layer of molecules covering the solid surfaces.

The Langmuir isotherm assumes that the adsorbed gas behaves as an ideal gas under isothermal conditions. Hence, there is a dynamic equilibrium at constant temperature and pressure between the adsorbed and non-absorbed gas.

Freeman et al. (2012) and Chao et al. (1994) concurred that instantaneous equilibrium of the sorbing surfaces and the storage in the pore space is assumed to be established under the Langmuir isotherm.

According to Freeman et al. (2012), this means there is no transient lag between pressure drop and desorption response when considered under modelling perspective.

Chao et al. (1994) concluded that due to the very low permeability of the shale, flow through the media is extremely slow and hence the assumption of instantaneous equilibrium is justified.

Langmuir isotherm is given by the formulae:

$$V = \frac{V_L P}{P + P_L}, \tag{2.15}$$

where V the volume of adsorbed gas at pressure P, V_L is the Langmuir volume or maximum gas adsorption at infinite pressure and P_L is the Langmuir pressure

corresponding to one half of the Langmuir volume. This formula will give the volume of adsorbed gas in scf/ft^3. In order to convert the gas content from scf/ft^3 to scf/ton, the bulk density of shale is needed.

The contribution of adsorbed gas to overall gas recovery has been modelled by various researchers in an effort to ascertain the role adsorption and desorption play in the recovery process. According to Cipolla et al. (2010), the contribution from adsorbed gas made up a low percentage of the overall gas recovery due to the ultra-low permeability of the rock. He also observed that the impact of desorption decreases when the network fracture spacing is smaller using the Barnett shale play. Accroding to their study, it is expected that gas adsorption will play a small role in the well performance with the desorption mainly occuring at the later life of the well when pressures in the tight matrix have become very low. Frantz et al. (2005) also concluded that in the Barnett shale, desorption is a less important factor in evaluating the well performance.

Mengal and Wattenbarger (2011) developed a shale gas pseudo-steady state model (SGPSS) to describe the contribution of adsorption on the life of the field and the calculation of original gas in place (OGIP). They found that incorporating the adsorbed gas to the model results in a 30% increase in OGIP and a 17% decrease in recovery factor. Stimulated reservoir volume estimates were found to be 5% less when adsorbed gas is considered. Mengal and Wattenbarger (2011) also pointed out that adsorption has little contribution during early times but contributes significantly at late times and low reservoir pressures.

Stephen Brunauer, P. H. Emmet and Edward Teller developed the BET isotherm in 1938 in which they assumed that the adsorption layers on the surface of the organic carbon were infinite. Unlike the Langmuir isotherm which assumed a monolayer adsorption, BET isotherm extended Langmuir's application to include a multi-layer adsorption. See Fig. 2.10 for the difference between single-layer and multi-layer adsorption.

With several key assumptions such as homogeneous surface, no lateral interactions between molecules and saturation pressure conditions, the number of layers becomes infinite. BET isotherm is considered a better fit to describing the adsorption processes in shale gas reservoir.

BET isotherm is classified as Type 2 isotherm which occurs in a non-porous or a macro-porous material (Kuila and Prasad 2013). The general form of the BET isotherm can be given as

$$V(P) = \frac{V_{\mathrm{m}} C \frac{P}{P_O}}{1 - \frac{P}{P_O}} \left[\frac{1 - (n+1)\left(\frac{P}{P_O}\right)^n + n\left(\frac{P}{P_O}\right)^{n+1}}{1 + (C-1)\frac{P}{P_O} - C\left(\frac{P}{P_O}\right)^{n+1}} \right] \tag{2.16}$$

V_{m} is the maximum adsorption gas volume when the entire adsorbent surface is being covered with a complete monolayer, C is a constant related to the net heat of adsorption, P_O is the saturation pressure of the gas and n is the maximum number of

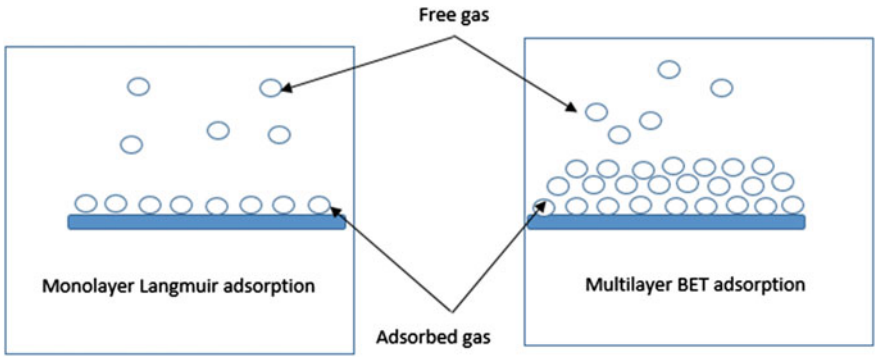

Fig. 2.10 Monolayer and multi-layer Langmuir isotherm

adsorption layers. When $n = 1$, the equation will be reduced to the Langmuir isotherm and when $n = \infty$, the equation reduces to

$$V_{\mathrm{L}} = \frac{V_{\mathrm{m}} CP}{(P_o - P)\left[1 + \frac{(C-1)P}{P_o}\right]} \tag{2.17}$$

A comparison of Langmuir and BET isotherm is shown in Fig. 2.11.

Yu et al. (2015) described for the first time that methane adsorption in shale gas reservoir behaved similar to multi-layer adsorption. Core samples from Marcellus shale were analysed and found to deviate from Langmuir isotherm but obey the Brunaeur-Emmett-Teller (BET) isotherm.

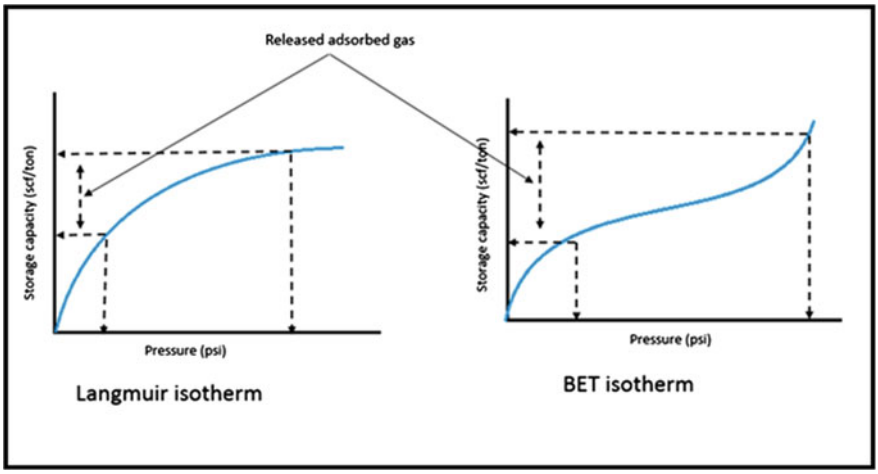

Fig. 2.11 Comparison of Langmuir and BET isotherms

Yu et al. (2015) also found that gas adsorption obeying the BET isotherm contributes to more production than gas adsorption obeying the Langmuir isotherm. They also argue that at very high pressures, the gas that is finally sorbed on the organic carbon surfaces forms multi-molecular layers and Langmuir isotherm may not be a good approximation of the amount of gas stored on the surfaces of the organic carbon.

Pure methane might not be the only component adsorbed on shale, with the presence of carbon dioxide, nitrogen and other heavier components. The presence of CO_2 with methane in the free gas makes the gas desorption behaviour and measurement most difficult. There is always competition for the same adsorption site by the components. Thus, the total volume of any of the gas will be less when they act independently.

Thus, the presence of more than one component within the pore network means that a better and more representative isotherm model will have to be taken into account.

Leahy-dios et al. (2011) suggested the use of multi-component adsorption isotherm model. According to Leahy-dios et al. (2011), a general form of expressing the multi-component adsorption is the extended Langmuir isotherm. They conducted experiments on the effect of multi-component adsorption and desorption on estimation and calculation of OGIP by using the extended Langmuir isotherm. By proposing a new multi-component adsorption model that allows the binary interaction parameters to capture non-ideal adsorption and also the fitting of adsorption isotherms for multi-component data sets, cumulative gas production could be increased by 10% over the life of the well.

Ambrose et al. (2011) also proposed a multi-component adsorption model that can be used to determine the composition and the amount of an adsorbed phase that is present. The extended Langmuir isotherm was chosen among other multi-component adsorption models such as ideal adsorbed solution (IAS) and the 2D equation of state (2D EOS) due to its wider use in the petroleum industry. Ambrose et al. (2011) proposed a new gas in place equation that combined the extended Langmuir model with volumetrics and the free gas composition; this method of calculating the gas in place showed a 20% decrease in gas in place compared with when the conventional approach was used in the calculation.

Ruthven (1984) proposed a general equation that represents the extended Langmuir isotherm as

$$V_{\mathrm{ads},i} = \frac{V_{\mathrm{L},i}\left(\frac{p_i}{p_{\mathrm{L},i}}\right)}{1 + \sum\left(\frac{p_i}{p_{\mathrm{L},j}}\right)} \tag{2.18}$$

where $V_{\mathrm{L},i}$ the Langmuir volume for component is i, $p_{\mathrm{L},i}$ is the Langmuir pressure component for i and $\sum\left(\frac{p_i}{p_{\mathrm{L},j}}\right)$ is the summation of all component pressure ratios i and j, p_i is the partial pressure of component i.

2.5 Stress-Dependent Permeability in Shale

In modelling of shale gas reservoirs, it is important to consider permeability changes due to overburden pressure. Very often in conventional reservoirs where the rocks are assumed permeable, permeability is modelled as insensitive to the effective pressure as the large pore throats of the rocks may not see a complete closure when effective pressure increases (Faulkner and Rutter 1998).

However, for unconventional reservoirs such as shale gas, the small grain size and pore spaces mean that they are easily affected by the influence of pressure. Thus, pressure changes throughout the reservoir have the effect of changing the permeability of the formation. The pore spaces can eventually be closed under effective pressure (i.e. Total pressure–Pore fluid pressure).

Previous modelling of shale gas reservoirs neglected the effect of stress-dependent fracture permeability on well productivity and gas recovery (Cipolla et al. 2009a). Cipolla et al. (2009b) showed the impact of closure stress and Young's modulus on unpropped fracture conductivity. Fracture conductivity decreased considerably as the closure stress increased and with decreasing Young's modulus. They conducted a number of simulation using Barnett shale properties and demonstrated the more severe effect of stress-dependent fracture conductivity on reducing gas recovery. According to them, for shales of lower Young's modulus, the corresponding increase in the closure stress and its effect on the fracture conductivity will be greater.

Pedrosa (1986) obtained pressure transient response in stress-sensitive formations by analytically solving the radial flow equation with pressure-dependent rock properties. In his model, he considered the reduction in permeability as a result of increase in effective stress. A new parameter known as the permeability modulus was included in his model to account for the permeability dependence on pressure. This permeability modulus is the fractional change in permeability with a unit change in pressure.

Lowering pore pressure has the effect of increasing the effective stress in the formation, and with low-permeability reservoirs, this has a major impact on the permeability of the formation. Thus, an essential feature of low-permeability reservoirs and fractured rocks is their sensitivity to effective stress in terms of both porosity and permeability (Pedrosa 1986).

Vairogs et al. (1971) conducted experimental studies to demonstrate that low-permeability reservoirs exhibit a much greater permeability reduction than reservoirs with much higher permeability. The authors proposed a mathematical model that incorporated the effect of stress on the permeability of tight reservoirs and used this model to predict production performance as a result of the effect of stress on the permeability of tight rocks.

Raghavan and Chin (2002) presented correlations in order to assess the production loss in stress-dependent permeability reservoirs. They believed that these correlations could be easily incorporated into reservoir simulators to do production forecasts and account for productivity changes. A rigorous mathematical model was

developed that combines geo-mechanical and fluid flow to correlate reductions that occur in production with time. They used three fundamental principles of linear momentum, mass conservation and Darcy's law in their model to compute pressure responses. The results from their studies showed that a high drawdown pressure, high overburden stress and an initially low reservoir pressure will increase stress-induced loss in productivity.

Cho et al. (2012) conducted a number of experimental studies to verify and calibrate existing pressure-dependent permeability correlations. These correlations were supported by a number of field examples and synthetic data with results indicating the loss of initial permeability of unpropped natural fractures following pressure depletion in the reservoir. Nevertheless, the authors cautioned against the use of fracture closure with pressure drop data without considering the complex interactions between the natural fractures and the shale matrix. A table of the correlations used in the studies of Cho et al. (2012) are presented (see Table 2.3).

Best and Katsube (1995) stated that there is no agreement on whether the relationship between permeability and pressure could be represented by a single mathematical expression. They, however, postulated that this relationship between pressure and permeability for shale can be expressed exponentially by the form

Table 2.3 Table of selected correlations (Cho et al. 2012)

	References	Correlation
1.	Rutqvist et al. (2002)	$k_f = k_{fi}\mathrm{e}^{c_1\left(\frac{\phi}{\phi_i}-1\right)}$, $\phi = \phi_{r1} + (\phi_i - \phi_{r1})\mathrm{e}^{a1\Delta p}$
2.	Rutqvist et al. (2002)	$k = k_{\mathrm{i}}F_k$, $F_k = \frac{\left[b_{\max 2}\left(\mathrm{e}^{d_2 d_y} - \mathrm{e}^{d_2\sigma' yi}\right)\right]^3 + \left[b_{\max 2}\left(\mathrm{e}^{d_2 d_z} - \mathrm{e}^{d_2\sigma' zi}\right)\right]^3}{b_{i2}^3 + b_{i2}^3}$
3.	Raghavan and Chin (2002) (rock type I)	$k_f = k_{fi}\mathrm{e}^{-d_{f3}\Delta p}$
4.	Raghavan and Chin (2002) (rock type II)	$k_f = k_{fi}\left(1 - m_{f4}\Delta p\right)$
5.	Raghavan and Chin (2002) (rock type III)	$k_f = k_{fi}\left(\frac{\phi_f}{\phi_{fi}}\right)^n$ with $\phi_f^{n+1} = 1 - \frac{1-\phi_f^n}{\mathrm{e}^{\Delta\varepsilon_v}}$, $\Delta\varepsilon_v = \frac{\alpha_5\Delta p(1+v_5)(2v_5-1)}{E_5(1-v_5)}$
6.	Raghavan and Chin (2002) and Celis et al. (1994)	$k_f = k_{fi}\left(\frac{\phi_f}{\phi_{fi}}\right)^n$, $\phi_f = \phi_{fi}\mathrm{e}^{-d_{f6}\Delta p}$
7.	Raghavan and Chin (2002) and Rutqvist et al. (2002)	$k_f = k_{fi}\left(\frac{\phi_f}{\phi_{fi}}\right)^n$, $\phi_f = \phi_{fi}F_\phi$, $F_\phi = \frac{b_1+b_2+b_3}{b_{1i}+b_{2i}+b_{3i}}$, $b = b_{f7} + b_{\max 7}\left[\mathrm{e}^{d_{f7}\sigma' n} - \mathrm{e}^{d_{f7}\sigma' ni}\right]$
8.	Raghavan and Chin (2002) and Minkoff et al. (2003)	$k_f = k_{fi}\left(\frac{\phi_f}{\phi_{fi}}\right)^n$, $\phi_f = \phi_{fi}\left(1 - m_{f8}\Delta p\right)$
9.	Raghavan and Chin (2002) and Minkoff et al. (2003)	$k_f = k_{fi}\left(\frac{\phi_f}{\phi_{fi}}\right)^n$, $\phi = 1 - \frac{(1-\phi_i)}{\mathrm{e}^{\varepsilon_v}}$, $\varepsilon_v = \frac{\alpha_g\Delta p\left(1+v_g\right)\left(2v_g-1\right)}{E_g\left(1-v_g\right)}$

$$k = k_o e^{-\alpha P_e} \tag{2.19}$$

where k_o is the permeability at atmospheric condition, P_e is the effective pressure and α is the slope of the curve of permeability versus effective pressure.

Gutierrez et al. (2000) conducted experimental studies to describe how fracture permeability varies with mechanical loading and to determine whether mechanical deformation can completely close a hydraulic fracture. The results from the experiments showed reduction in fracture permeability when increasing normal stress. But they observed that the fracture is never completely closed under this stress and the permeability remained higher compared to the shale matrix permeability.

Franquet et al. (2004) noted that substantial errors are likely to be obtained if proper appreciation of the mechanics of rock compressibility under various states of stress is not examined. Pressure-dependent permeability data are very rare to come by and hence most analysis of permeability in well test analysis is done with the assumption of a constant permeability. They attempted to evaluate the error caused by ignoring the pressure-dependent permeability in tight gas reservoirs by simulating the pressure-dependent permeability using an exponential form for the permeability versus pressure drop. This simulation model, therefore, required only one parameter γ which is the permeability modulus, psia^{-1}.

$$k = k_i e^{-\gamma(p_i - p)} \tag{2.20}$$

k, k_i are the current and initial permeability, respectively, while p, p_i are the current and initial pressures.

Navarro (2012) conducted field studies of wells in Robore III reservoir, Bolivia, to investigate the decline in production by analysing compressibility, production and pressure data. It was found that production decline was primary as a result of the closure of fractures due to an increase in the effective stress. The closure of the natural fractures leads to the reservoir becoming more of a matrix permeability reservoir.

Tao et al. (2009) conducted numerical modelling combining a fully coupled poro-elastic displacement discontinuity method and nonlinear fracture deformation model to analyse the change in fracture permeability in fractured reservoirs. Their studies focussed on fractures since they are susceptible to change under stress compared to that of the matrix. Their work showed that fracture permeability reduces due to the increases in effective normal stress. Thus under isotropic stress conditions, fracture permeability was found to be decreasing. According to Tao et al. (2009), fracture permeability may increase during production especially in high anisotropic stress.

Wu and Pruess (2000) presented integral solutions for transient flow through a porous media by considering pressure-dependent permeability. They observed the effects of pressure on permeability by using integral solutions for one-dimensional

single-phase, slightly compressible linear and radial flow through a horizontal fracture. The results of their studies also showed that ignoring pressure dependence on permeability may lead to significant errors in flow behaviour under high-pressure operations.

Berumen and Tiab (1996) presented new numerical approach for interpreting the effect of permeability changes in artificially fractured rocks. By considering non-linear effect of pressure dependence, new type curves were generated for pressure sensitive fracture formations. The use of conventional techniques in evaluating fractured wells was found to be insufficient and led to inaccurate estimates.

According to Wheaton (2017), there has been no analytically derived relationship that relates shale permeability to pressure and geo-mechanical properties. Wheaton (2017), therefore, tried to examine the theoretical dependence of shale permeability on pressure and geo-mechanical properties of shale using Young's modulus and poison ratio. By developing a simple equation to relate shale permeability to pressure, Young's modulus and poison ratio, he was able to predict shale permeability on the basis of geo-mechanical properties.

$$\frac{k(p_i)}{k(p_o)} = \left[1 + \frac{3p_i(1-2v)}{E\phi_o}\right]^3 \tag{2.21}$$

where p_i = initial producing pressure, $k(p_o)$ = shale permeability under surface conditions and $k(p_i)$ = estimated shale permeability under initial production conditions. Also E, v represents Young's modulus and poison ratio, respectively.

The model equation though cannot be verified due to the absence of any experimental data which relates the dependence of shale permeability to pressure as a function of Young's modulus and poison ratio in shale.

References

Adachi J, Siebrits E, Peirce A, Desroches J (2007) Computer simulation of hydraulic fractures. Int J Rock Mech Min Sci 44:739–757. https://doi.org/10.1016/j.ijrmms.2006.11.006

Akkutlu IY, Fathi E (2011) Gas transport in shales with local kerogen heterogeneities. In: SPE annual technical conference and exhibition. SPE 146422, p 13. https://doi.org/10.2118/146422-MS

Ambrose RJ, Hartman RC, Labs W, Akkutlu IY (2011) Multi-component sorbed-phase considerations for shale gas-in-place calculations. In: SPE production and operations symposium. SPE 141416, pp 1–10. https://doi.org/10.2118/141416-MS

Azom PN, Javadpour F (2012) Dual continuum Modeling of shale and tight gas reservoirs. Society of petroleum engineers. doi:10.2118/159584-MS

Bai M, Elsworth D, Roegiers JC (1993) Modeling of naturally fractured reservoirs using deformation dependent flow mechanism. In: International journal of rock mechanics and mining sciences & geomechanics abstracts. 30(7):1185–1191. Pergamon

Barenblatt GI, Zheltov IP, Kochina IN (1960) Basic concepts in the theory of seepage of homogeneous liquids in fissured rocks [strata]. J Appl Math Mech 24:1286–1303

Berumen S, Tiab D (1996) Effect of pore pressure on conductivity and permeability of fractured rocks. In: Proceedings of SPE western regional meeting, pp 445–460. https://doi.org/10.2523/35694-MS

Beskok A, Karniadakis GE (1999) A model for flows in channels, pipes, and ducts at micro and nano scales. Microscale Thermophys Eng 3:43–77. https://doi.org/10.1080/108939599199864

Best ME, Katsube TJ (1995) Shale permeability and its significance in hydrocarbon exploration. Lead. Edge 14:165–170. https://doi.org/10.1190/1.1437104

Celis V, Silva R, Ramones M, Guerra J, Da Prat G (1994) A New Model for Pressure Transient Analysis in Stress Sensitive Naturally Fractured Reservoirs. Soc Pet Eng doi:10.2118/23668-PA

Chen L, Zhang L, Kang Q, Yao J, Tao W (2015) Nanoscale simulation of shale transport properties using the lattice Boltzmann method: permeability and diffusivity Li Chen. Sci Rep 25(7):134–139

Chao C, Lee J, Spivey JP, Semmelbeck ME (1994) Modeling multilayer gas reservoirs including sorption effects. Society of Petroleum Engineers. doi:10.2118/29173-MS

Cho Y, Apaydin O, Ozkan E (2012) Pressure-dependent natural-fracture permeability in shale and its effect on shale-gas well production. Soc Pet Eng. SPE 159801, 1–18. https://doi.org/10.2118/159801-PA

Cipolla C, Lolon E, Erdle J, Rubin B (2010) Reservoir modeling in shale-gas reservoirs. SPE Reserv Eval Eng 13:23–25. https://doi.org/10.2118/125530-PA

Cipolla CL, Lolon E, Mayerhofer MJ, Warpinski NR (2009a) Fracture Design Considerations in Horizontal Wells Drilled in Unconventional Gas Reservoirs. Soc Pet Eng. doi:10.2118/119366-MS

Cipolla CL, Lolon EP, Erdle JC, Tathed V (2009b) Modeling well performance in shale-gas reservoirs. SPE 125532, pp 19–21. https://doi.org/10.2118/125532-MS

Civan F (2010) Effective correlation of apparent gas permeability in tight porous media. Transp Porous Media 82:375–384. https://doi.org/10.1007/s11242-009-9432-z

Clarkson CR, Haghshenas B (2013) Modeling of supercritical fluid adsorption on organic-rich shales and coal. In: SPE unconventional resources conference, pp 1–24. https://doi.org/10.2118/164532-MS

Daneshy AA (1973) On the design of vertical hydraulic fractures. J Pet Technol 25:83–97. https://doi.org/10.2118/3654-PA

Darabi H, Ettehad A, Javadpour F, Sepehrnoori K (2012) Gas flow in ultra-tight shale strata. J Fluid Mech 710:641–658. https://doi.org/10.1017/jfm.2012.424

de Swaan OA (1976) Analytic solutions for determining naturally fractured reservoir properties by well testing. https://doi.org/10.2118/5346-PA

Dershowitz WS, La Pointe PR, Doe TW et al (2004) Advances in discrete fracture network modeling. In: Proceedings of the US EPA/NGWA fractured rock conference, Portland, pp 882–894

Faulkner DR, Rutter EH (1998) The gas permeability of clay-bearing fault gouge at 20 °C. Geol Soc London Spec Publ 147:147–156. https://doi.org/10.1144/gsl.sp.1998.147.01.10

Franquet M, Ibrahim M, Wattenbarger R, Maggard J (2004) Effect of pressure-dependent permeability in tight gas reservoirs, transient radial flow. Proc Can Int Pet Conf, 1–10. https://doi.org/10.2118/2004-089

Frantz J, Sawyer W, MacDonald R, Williamson J, Johnston D, Waters G (2005) Evaluating barnett shale production performance using an integrated approach. Proc SPE Annu Tech Conf Exhib, 1–18. https://doi.org/10.2523/96917-MS

Freeman C, Moridis GJ, Michael GE, Blasingame TA (2012) Measurement, modeling, and diagnostics of flowing gas composition changes in shale gas wells. SPE 153391. doi:10.2118/153391-MS

Gad-el-hak M (1999) The fluid mechanics of microdevices—the freeman scholar lecture. Transactions-American Society of Mechanical Engineers Journal of FLUIDS Engineering, 121:5–33

Geertsma J, De Klerk F (1969) A rapid method of predicting width and extent of hydraulically induced fractures. J Pet Technol 21:1571–1581. https://doi.org/10.2118/2458-PA

Geng L, Li G, Zitha P, Tian S, Sheng M, Fan X (2016) A diffusion–viscous flow model for simulating shale gas transport in nano-pores. Fuel 181:887–894. https://doi.org/10.1016/j.fuel.2016.05.036

Guo C, Xu J, Wu K, Wei M, Liu S (2015) Study on gas flow through nano pores of shale gas reservoirs. Fuel 143:107–117. https://doi.org/10.1016/j.fuel.2014.11.032

Gutierrez M, Øino LE, Nygård R (2000) Stress-dependent permeability of a de-mineralised fracture in shale. Mar Pet Geol 17:895–907. https://doi.org/10.1016/S0264-8172(00)00027-1

Herbert AW (1996) Modelling approaches for discrete fracture network flow analysis. Dev Geotech Eng 79:213–229

Howard G, Fast CR (1957) Optimum fluid characteristics for fracture extension? In: Proceedings of American Petroleum Institute, pp 261–270. API-57-261

Javadpour F (2009) Nanopores and apparent permeability of gas flow in mudrocks (Shales and Siltstone). Soc Pet Eng J 48:1–6. https://doi.org/10.2118/09-08-16-DA

Javadpour F, Fisher D, Unsworth M (2007) Nanoscale gas flow in shale gas sediments. J Can Pet Technol 46:55–61. https://doi.org/10.2118/07-10-06

Kazemi H (1969) Pressure transient analysis of naturally fractured reservoirs with uniform fracture distribution. https://doi.org/10.2118/2156-A

Kelly S, El-Sobky H, Torres-Verdín C, Balhoff MT (2015) Assessing the utility of FIB-SEM images for shale digital rock physics. Adv Water Resour, 1–15. https://doi.org/10.1016/j.advwatres.2015.06.010

Klinkenberg LJ (1941) The permeability of porous media to liquids and gases. Drilling and production practice, pp 200–213. American Petroleum Institute

Kuila U, Prasad M (2013) Specific surface area and pore-size distribution in clays and shales. Geophys Prospect 61:341–362. https://doi.org/10.1111/1365-2478.12028

Leahy-dios A, Das M, Agarwal A, Kaminsky RD, Upstream E (2011) Modeling of transport phenomena and multicomponent sorption for shale gas and coalbed methane in an unstructured grid simulator adsorbed gas, scf/tonne. SPE Annu, 1–9. https://doi.org/10.2118/147352-MS

Lee KS, Kim TH (2015) Integrative understanding of shale gas reservoirs, 1st edn. Springer, Berlin. https://doi.org/10.1007/978-3-319-29296-0

Mack MG, Warpinski NR (2000) Mechanics of hydraulic fracturing. Reservoir stimulation. MJ Economides and KG Nolte

Martin JP, Hill DG, Lombardi TE, Nyahay R (2010) A Primer on New York's gas shales, pp 1–32

McCabe WJ, Barry BJ, Manning MR (1983) Radioactive tracers in geothermal underground water flow studies. Geothermics 12:83–110

McClure M, Horne RN (2013) Discrete fracture network modeling of hydraulic stimulation: coupling flow and geomechanics. Springer, Berlin

Mehmani A, Prodanović M, Javadpour F (2013) Multiscale, multiphysics network modeling of shale matrix gas flows. Transp Porous Media 99:377–390. https://doi.org/10.1007/s11242-013-0191-5

Mengal SA, Wattenbarger RA (2011) Accounting for adsorbed gas in shale gas reservoirs. SPE Conf, 25–28. https://doi.org/10.2118/141085-MS

Minkoff SE, Stone CM, Bryant S, Peszynska M, Wheeler MF (2003) Coupled fluid flow and geomechanical deformation modeling. J Petrol Sci Eng. 38(1):37–56

Moghaddam R, Jamiolahmady M (2016) Slip flow in porous media. Fuel 173:298–310. https://doi.org/10.1016/j.fuel.2016.01.057

Myong RS (2003) Gaseous slip models based on the Langmuir adsorption isotherm. Phys Fluids 16:104–117. https://doi.org/10.1063/1.1630799

Najurieta HL (1980) A theory for pressure transient analysis in naturally fractured reservoirs. https://doi.org/10.2118/6017-PA

Naraghi ME, Javadpour F (2015) A stochastic permeability model for the shale-gas systems. Int J Coal Geol 140:111–124. https://doi.org/10.1016/j.coal.2015.02.004

Navarro VOG (2012) Closure of natural fractures caused by increased effective stress, a case study: Reservoir Robore III, Bulo Bulo Field, Bolivia. Soc Pet Eng. SPE 153609, 1–11. https://doi.org/10.2118/153609-MS

Nordgren RRP (1972) Propagation of a vertical hydraulic fracture. Soc Pet Eng J 12:306–314. https://doi.org/10.2118/3009-PA

Odeh AS (1965) Unsteady-state behavior of naturally fractured reservoirs. https://doi.org/10.2118/966-PA

Pedrosa OA (1986) Pressure transient response in stress-sensitive formations. SPE 15115. https://doi.org/10.2118/23312-MS

Perkins TK, Kern LR (1961) Widths of hydraulic fractures. J Pet Technol 13:937–949. https://doi.org/10.2118/89-PA

Raghavan R, Chin LY (2002) Productivity changes in reservoirs with stress-dependent permeability. Soc Pet Eng. SPE 88870, 308–315. https://doi.org/10.2118/77535-MS

Rahman MM, Rahman MK (2010) A review of hydraulic fracture models and development of an improved pseudo-3D model for stimulating tight oil/gas sand. Energy Sources Part A Recover Util Environ Eff 32:1416–1436. https://doi.org/10.1080/15567030903060523

Rathakrishnan E (2013) Gas dynamics. PHI Learning Pvt. Ltd, New Delhi

Rezaveisi M, Javadpour F, Sepehrnoori K (2014) Modeling chromatographic separation of produced gas in shale wells. Int J Coal Geol 121:110–122. https://doi.org/10.1016/j.coal.2013.11.005

Ruthven DM (1984) Principles of adsorption and adsorption processes. John Wiley & Sons

Rutqvist J, Wu YS, Tsang CF, Bodvarsson G (2002) A modeling approach for analysis of coupled multiphase fluid flow, heat transfer, and deformation in fractured porous rock. Int J Rock Mech Min Sci 39(4):429–442

Sakhaee-pour A, Bryant SL (2011) Gas Permeability of Shale. Soc Pet Eng. doi:10.2118/146944-MS

Serra K, Reynolds AC, Raghavan R (1983) New pressure transient analysis methods for naturally fractured reservoirs. https://doi.org/10.2118/10780-PA

Settari A, Cleary MP (1986) Development and testing of a pseudo-three-dimensional model of hydraulic fracture geometry. SPE Prod Eng 1:449–466. https://doi.org/10.2118/10505-PA

Shabro V, Torres-Verdín C, Javadpour F, Sepehrnoori K (2012) Finite-difference approximation for fluid-flow simulation and calculation of permeability in porous media. Transp Porous Media 94:775–793. https://doi.org/10.1007/s11242-012-0024-y

Singh H, Javadpour F (2015) Langmuir slip-Langmuir sorption permeability model of shale. Fuel 164:28–37. https://doi.org/10.1016/j.fuel.2015.09.073

Singh H, Javadpour F (2016) Langmuir slip-Langmuir sorption permeability model of shale. Fuel, 164:28–37

Tao Q, Ehlig-Economides CA, Ghassemi A (2009) Investigation of stress-dependent fracture permeability in naturally fractured reservoirs using a fully coupled poroelastic displacement discontinuity model. Proc SPE Annu Tech Conf Exhib 5:2996–3003. https://doi.org/10.2118/124745-MS

Vairogs J, Hearn CL, Dareing DW, Rhoades VW (1971) Effect of rock stress on gas production from low-permeability reservoirs. Soc Pet Eng 5:1161–1167. https://doi.org/10.2118/3001-PA

Walton I, Mclennan J (2013) The role of natural fractures in shale gas production. https://doi.org/10.5772/56404

Warren JEE, Root PJJ (1963) The behavior of naturally fractured reservoirs. Soc Pet Eng J 3:245–255. https://doi.org/10.2118/426-PA

Weng X (2015) Modeling of complex hydraulic fractures in naturally fractured formation. J Unconv Oil Gas Resour 9:114–135. https://doi.org/10.1016/j.juogr.2014.07.001

Wheaton R (2017) Dependence of shale permeability on pressure. Society of petroleum engineers. doi:10.2118/183629-PA

Wu Y-S, Pruess K (2000) Integral solutions for transient fluid flow through a porous medium with pressure-dependent permeability. Int J Rock Mech Min Sci 37:51–61. https://doi.org/10.1016/S1365-1609(99)00091-X

Yew CH, Weng X, Yew CH, Weng X (2015) Fracturing of a wellbore and 2D fracture models (Chapter 1). In: Mechanics of hydraulic fracturing, pp 1–22. https://doi.org/10.1016/B978-0-12-420003-6.00001-X

Yu W, Sepehrnoori K, Patzek TW (2014) Evaluation of gas adsorption in marcellus shale. Society of petroleum engineers. pp 27–29. doi:10.2118/170801-MS

Yu W, Sepehrnoori K, Patzek TW (2015) Modeling gas adsorption in marcellus shale with Langmuir and BET isotherms. SPE J. https://doi.org/10.2118/170801-PA

http://www.springer.com/978-3-319-70768-6

Challenges in Modelling and Simulation of Shale Gas Reservoirs

Gholinezhad, J.; Fianu, J.S.; Galal Hassan, M.

2018, XIII, 84 p. 37 illus., 33 illus. in color., Softcover
ISBN: 978-3-319-70768-6